Sensitivity analysis of CFD coupled non-isothermal heat and moisture modelling

In: Building and Environment, 45 (11), pp. 2485-2496, 2010.

Sensitivity analysis of CFD coupled non-isothermal heat and moisture modelling

Marnix Van Belleghem[1], Hendrik-Jan Steeman[1], Marijke Steeman[2], Arnold Janssens[2], Michel De Paepe[1]

[1]Department of Flow Heat and Combustion Mechanics, Ghent University, Sint-Pietersnieuwstraat 41, 9000 Ghent, Belgium
[2]Department of Architecture and Urban Planning, Ghent University, Jozef Plateaustraat 22, 9000 Ghent, Belgium

Corresponding author:
Tel +3292643289 / Fax +3292643575
Email: marnix.vanbelleghem@UGent.be

Abstract
CFD (Computational Fluid Dynamics) is a useful tool to study air flow patterns in a room. Current CFD models are able to simulate air flow combined with temperature distributions and species distributions. In this paper a coupled CFD-HAM model is discussed. This model combines CFD with a HAM model (Heat, Air and Moisture) for hygroscopic materials. This coupled model is able to simulate air flow around a porous material and combines this with heat and moisture transport in the porous material. Validation with a small scale experiment in which gypsum board was used as a hygroscopic material showed good results. In this paper a further validation of the model is discussed based on a sensitivity analysis of some model parameters. Especially hygrothermal parameters like sorption isotherm and water vapour permeability proved to have a non negligible influence on the modelling outcome. Adding a hysteresis model showed improvement of the model during desorption. The model was also used to compare two modelling strategies. In one strategy the gypsum board was modelled as a uniform material, in a second approach the material was modelled as being layered. The difference between the two approaches showed to be negligible.

Keywords: CFD, heat and moisture transport, modelling, sensitivity, non-isothermal

1. Introduction
Temperature and relative humidity are two important parameters for damage risk assessment of buildings. E.g. too high levels of indoor relative humidity can cause mould growth on the inside surfaces of the building envelope. When moisture migrates through the building envelope, interstitial condensation can occur which can lead to rot, deterioration of outside surfaces or other damage phenomena. Even if humidity levels are kept low enough, damage can still occur due to too strong variations. E.g. paintings and artefacts can show cracks when exposed to fluctuating temperatures and humidity levels [1]. Having a good knowledge of the heat, air and moisture transport in a building is also of great importance for many other applications. Moisture buffering by hygroscopic materials levels out indoor relative humidity fluctuations. This can reduce the energy use

of HVAC systems [2] and improve the perceived indoor air quality at the same time [3]. In literature some examples are found where the importance of knowing the relative humidity in the design stage of a HVAC system is highlighted [4,5].
Buildings are complex systems and can be studied at different levels (whole buildings, rooms, building components…). Therefore, depending on the application, Heat, Air and Moisture transfer (HAM) in buildings is modelled through different approaches and a lot of different modelling tools are being developed. Overviews of recent developed HAM models are found in [6] and [7].
A new trend in HAM modelling is the coupling of these models to BES (building energy simulation) models or CFD (Computational Fluid Dynamics) models depending on the application aimed at. Both modelling approaches were evaluated by Steeman et al. [8]. Coupling HAM models with BES is useful when the impact of moisture on energy use in a building is studied. Examples of such modelling approaches are found in [9,10]. Kwiatkowski et al. [9] used an isothermal modelling approach and neglected the latent heat in the porous material, where Steeman et al. [10] added this to their model. Combining CFD with a HAM model is interesting when a detailed study of the air flow field around a hygroscopic object is needed. For example microclimates can occur near artefacts. A detailed study of these microclimates is necessary for the assessment of damage risks [11, 12].
Most BES programs are typically multizone models: they represent a room as one node and have the assumption that state variables (e.g. temperature, relative humidity…) are uniform for the entire zone (well-mixed air assumption). The coupling between the HAM model and the BES model is accomplished by using transfer coefficients. The heat transfer coefficient is used to model the heat transfer (convective and radiant) between the environment and the surface of the porous material (walls, furniture…). The mass transfer coefficient models the moisture transfer between the air and the porous material [13]. They have to be determined indirectly through empirical or analytical correlations or from CFD calculations. Often the heat and mass transfer analogy is used to convert heat transfer coefficients into mass transfer coefficients. Steeman et al. [14] however showed that this analogy does not always apply.
CFD on the other hand does not require transfer coefficients to model the interaction between the fluid and solid interface. At the same time CFD allows the analysis of complex geometries and provides detailed information on temperature and humidity distributions in the air. One major drawback of CFD is the high computational cost. Therefore, up till now, applications are limited to the study of microclimates and building details.
Whatever coupling approach is used, HAM models still need proper input data like boundary conditions, initial conditions and material property data. Extensive databases for these material properties can be found in literature [6, 15, 16]. However, recent studies revealed a large spread of some of these material properties when the same material was measured by different laboratories [16, 17]. It is often not clear how this will affect the model outcome.
This paper highlights the importance of a sensitivity analysis for newly developed coupled HAM models. These models need a lot of material property data as input which introduce uncertainty to the model outcome. Therefore an elaborate sensitivity analysis is performed on a recently developed coupled CFD-HAM model [12]. The first part of this

paper gives a brief description of the model. This model is then used to simulate air flow over a gypsum board surface. In the reference case predefined material properties are used. Afterwards different input parameters are evaluated based on a so-called One-at-a-Time sensitivity analysis. Also the air velocity, inlet temperature and humidity and the impact of hysteresis modelling are evaluated.
Finally uniform modelling of gypsum board is investigated. Gypsum board is built up out of layers (finishing paper and gypsum) but modelled with averaged material properties. This modelling approach is compared to an approach where each layer is modelled separately.

2. Model

Standard CFD packages do not include a HAM model to simulate the interaction with porous materials. Therefore a new model was added to an existing CFD package (Fluent®). This model is discussed more detailed in Steeman et al. [12]. In this paper only a short overview of the modelling approach is given.
Heat and moisture transfer in the air, porous material and at the interface is modelled in its full complexity. This makes the model very useful for the assessment of moisture related problems in microclimates.
A direct coupling approach is used. This implies that the computational domain encloses the air region as well as the porous material and both domains are solved by one and the same solver. Nevertheless, for each region (porous material or air) a different set of equations has to be solved.
By introducing the latent heat into the equations for heat transfer, the influence of phase change in the porous material is captured and the variation of temperature in the porous material can also be evaluated.

2.1. Heat and moisture transfer in the air

The air is modelled as an incompressible ideal gas. In this case the energy and moisture transport equations reduce to equations (1) and (2). Note that for the transported variables, temperature, T [K], is chosen for the energy equation and the mass fraction of water vapour, Y [kg/kg], for the moisture transport equation. The same transport variables are used in the transport equations for the porous material.

$$\frac{\partial}{\partial t}\left(\rho_{air} CT\right) + \nabla.\left(\vec{v}\rho_{air} CT\right) = \nabla.\left(\lambda_{air}\nabla\left(T\right) - \left(C_{vap} - C_{air}\right)\vec{g}T\right) \quad (1)$$

$$\frac{\partial}{\partial t}\left(\rho_{air} Y\right) + \nabla.\left(\rho_{air}\vec{v}Y\right) = \nabla.\left(\rho_{air} D\nabla\left(Y\right)\right) = -\nabla.\vec{g} \quad (2)$$

with

$$C = YC_{vap} + \left(1 - Y\right)C_{air} \quad (3)$$

In these equations ρ_{air} [kg/m³] is the density of the humid air, C_{vap} [J/kgK] is the specific heat capacity of water vapour, C_{air} [J/kgK] is the specific heat capacity of air and C [J/kgK] is the weighted average specific heat capacity according to equation (3), λ_{air} [W/mK] is the thermal conductivity of air and g [kg/m²s] the water vapour diffusion flux.

D [m²/s] is the diffusion coefficient of water vapour in air. The first term on the left hand side of each transport equation is the storage term, the second term represents the convective term while the right hand side represents the transport by diffusion.

2.2. Heat and moisture transfer in porous materials

For the porous material zone the following assumptions are made in the model:

- No air transfer occurs
- Liquid transfer is not dominant
- Moisture storage only depends on relative humidity
- The temperature remains below the boiling point
- There is no radiative transfer inside the porous material

The model is only valid in the hygroscopic range (RH <98%). Here moisture transfer by equivalent vapour diffusion is dominant. This implies that the moisture transfer can be modelled by a single water vapour diffusion coefficient. Equations (4) and (5) describe the moisture transfer and the heat transfer in the porous material. Again, temperature T and vapour mass fraction Y are used as the transported variables. Note how latent heat of vaporization L_{vap} (2.5×10^6 J/kg) appears in equation (5). Due to the capillary action of the porous material, part of the water vapour entering the porous material condenses, even at relative humidity lower than 100%. On the other hand liquid water evaporates from the pores when the porous material dries out. This phase change is accompanied by a latent heat effect. At low relative humidity (RH <40%), sorption and desorption are governed by adsorption of water molecules at the porous walls. This is accompanied by a heat of adsorption. For this model heat of sorption is assumed to be equal to the latent heat of vaporization. This assumption is often used in hygroscopic modelling [3].

$$\frac{dw}{dt} = -\nabla.\vec{g} \Leftrightarrow \frac{\partial w}{\partial RH}\frac{\partial RH}{\partial Y}\frac{\partial Y}{\partial t} + \frac{\partial w}{\partial RH}\frac{\partial RH}{\partial T}\frac{\partial T}{\partial t} = \nabla\left(\rho_{air}\frac{D}{\mu}\nabla(Y)\right) \tag{4}$$

$$\begin{aligned}\frac{dE}{dt} &= \nabla.\left(\lambda_{mat}\nabla(T) - \left(\left(C_{vap} - C_{air}\right)T + L_{vap}\right)\vec{g}\right) \Leftrightarrow \\ \rho_{mat}C\frac{\partial T}{\partial t} + C_{liq}T\frac{\partial w_{liq}}{\partial t} &+ \left(C_{vap}T + L_{vap}\right)\frac{\partial w_{vap}}{\partial t} = \nabla.\left(\lambda\ \nabla(T) - \left(\left(C_{vap} - C_{air}\right)T + L_{vap}\right)\vec{g}\right)\end{aligned} \tag{5}$$

with

$$E = \rho_{mat}C_{mat}T + C_{liq}w_{liq}T + \left(C_{vap}T + L_{vap}\right)w_{vap} \tag{6}$$

$$C = C_{mat} + \frac{C_{liq}w_{liq}}{\rho_{mat}} + \frac{C_{vap}w_{vap}}{\rho_{mat}} \tag{7}$$

$$w_{liq} = \frac{\phi - \frac{w}{\rho_{vap}}}{\frac{1}{\rho_{liq}} - \frac{1}{\rho_{vap}}} \tag{8}$$

$$w_{vap} = \frac{\frac{w}{\rho_{liq}} - \phi}{\frac{1}{\rho_{liq}} - \frac{1}{\rho_{vap}}} \tag{9}$$

In equations (4) to (9) *mat* refers to the dry material properties, *liq* stands for liquid water and *vap* for water vapour. In the material model described by equations (4) to (9) the following material properties have to be known: the sorption isotherm which states the relation between the equilibrium moisture content w [kg/m³] and the relative humidity RH, the vapour resistance factor μ [-] as a function of moisture content , the dry density ρ_{mat} [kg/m³], the heat capacity C_{mat} [J/kgK], the open porosity Φ [-] and the thermal conductivity λ [W/mK]. The vapour resistance factor can also be expressed as function of the relative humidity if no hysteresis is modelled. In that case a unique relationship between moisture content and relative humidity is assumed. The thermal conductivity λ combines the thermal conductivity of the dry material with the conductivity of the water captured in the material pore structure and is therefore a function of the moisture content. When no hysteresis is modelled it can be expressed as a function of the relative humidity. The liquid moisture content w_{liq} and the water vapour content w_{vap} in the porous material can be related to the total moisture content w through equations (8) and (9) taking into account that $w = w_{liq} + w_{vap}$ and $\Phi = w_{liq}/\rho_{liq} + w_{vap}/\rho_{vap}$.

3. Reference case

In order to perform a sensitivity analysis on the coupled CFD-HAM model, a proper reference case was selected. The same case was used by Steeman et al. [12] to validate the coupled CFD-HAM model. The case is based on an experimental setup discussed in detail by Talukdar et al. [18]. In this paragraph only a short description of the test facility is given.

Figure 1 shows a schematic representation of the reference case setup. Only the section of interest is shown. The figure represents a part of a wind tunnel. Preconditioned air enters the section on the right hand side with a fully developed air profile. This air flows over a sample of porous material. Gypsum board was used for this investigation. Three gypsum boards with a thickness of 12.5mm were stacked on top of each other. The gypsum boards have a length of 500mm and a width of 298mm. Only the top of the stack is in contact with the air duct, the other boundaries are assumed to be adiabatic. The cross section of the duct has a height of 20.5mm and a width of 298mm. Air enters the duct at a constant temperature. The samples were preconditioned at a low relative humidity (30%) and constant temperature (23.3°C). Afterwards the relative humidity was changed to a higher value (RH=71.9%, T=23.8°C) for 24 hours and then lowered again for 24 hours (RH=29.6%, T=22.5°C). Thermocouples and RH sensors were placed at a depth of

12.5mm and 25mm to measure temperature and relative humidity in the hygroscopic material.
The average air velocity in the duct was 0.82m/s which corresponds with a Reynolds number of 2000. The air was preconditioned before it entered the test section and an upstream developing section ensured a fully developed flow pattern. For the case of Re=2000 the airflow pattern was assumed to be laminar in accordance to [19].
A 2D structured grid was used, counting 33,800 rectangular cells. The grid was dense near the air material interface and gradually coarsened towards the bottom of the porous material and the centre of the duct. The grid dependency was investigated by using Richardson extrapolation [12]. The original grid was refined with a factor 2 and a factor 4 for both the X and Y direction and the mass flow through the interface was calculated. Using Richardson extrapolation the exact mass flow rate through the interface can be calculated out of the different mass flow rates for the different grid sizes. Because the difference between the exact value and the simulated value is less than 1% it can be assumed that the solution is grid independent. In order to reduce numerical diffusion a second order upwind scheme is used for the discretization of the convective terms. The PISO algorithm is used for the pressure-velocity coupling. To reduce the round-off errors, a double precision representation of real numbers is used.

4. Material properties

The material properties used for the reference case were taken from IEA Annex 41 [16]. These properties are needed to solve equations (4) to (9). Report 2 of Annex 41 comprises an elaborate round robin test for some of these porous material properties. Samples of the same gypsum board were sent to different laboratories where the material properties were determined. Figure 2 and 3 show the average sorption isotherm and vapour resistance factor calculated from the data of Annex 41 [16] together with the upper (w+) and lower (w-) measured values. The round robin test performed in subtask 2 of this Annex revealed large discrepancies in the sorption isotherm and vapour resistance factor measured by 14 laboratories. Differences up to 20% were found. It is expected that this will have an influence on the model outcome, since the accuracy of the solution is to a great extent determined by the accuracy of the input parameters.

Table 1 lists five properties of gypsum board used in the sensitivity analysis. For each property an upper and lower limit is determined, which corresponds to an increase or decrease of 5% of the original value. This is indicated in the table by Min(-5%) and Max(+5%). First, simulations are performed with the reference values. The output of these simulations is referred to as the reference case. The sensitivity analysis is performed by changing one property at a time (so-called One-at-a-Time analysis). Note that for this analysis the effect of density and open porosity is not evaluated independently: it is assumed that an increase of the open porosity by 5% would result in a decrease of the density by 5% and vice versa.

The properties listed in Table 1 are fairly easy to measure and can be often determined quite accurately. This is why Report 2 of Annex 41 [16] only includes a sensitivity analysis in which the effect of transfer coefficients, sorption isotherm and permeability was investigated. The influence of density, open porosity, heat capacity and thermal

conductivity was neglected. Nevertheless an uncertainty (though limited) can always be expected, which still justifies a sensitivity analysis for these parameters. Only a change of 5% is considered, which is still higher than the expected uncertainty.

To model the material properties as accurately as possible the following analytical functions are used to describe the sorption isotherm and the vapour resistance factor of gypsum board (Figure 2 and 3). The coefficients are determined by fitting the analytical functions to experimental data.

$$w_a = \frac{RH}{aRH^2 + bRH + c} \tag{10}$$

$$w_d = a\left(1 - \frac{\ln(RH)}{b}\right)^{-\frac{1}{c}} \tag{11}$$

$$\mu = \frac{\mu_0}{1 + aRH^n} \tag{12}$$

For the analysis with hysteresis at least two sorption isotherm curves are needed: w_a is the sorption curve during adsorption and w_d during desorption. The corresponding coefficients for equations (10) to (12) are listed in Table 2. For each function a set of coefficients is given for the average curve fit, for the lower curve (-) and for the upper curve (+). No sensitivity analysis was performed on the desorption isotherm, so for this curve only one set of coefficients is given.

5. Sensitivity analysis

Studies of [16] and [17] showed a large variability of measured material properties, which stresses the importance of a sensitivity analysis. The effect of changes in the material properties on the numerical results will be studied in this section. In total five material properties are studied: dry density (combined with open porosity), thermal conductivity, heat capacity, sorption isotherm and moisture permeability. The latter is represented here as a water vapour resistance factor. The material properties of air are assumed to be constant in the model and are not investigated here. Their effect on the model is assumed to be negligible compared to the variability of the porous material properties. The same counts for the latent heat of vaporization which is assumed to be constant in the model.

Temperature and relative humidity at a depth of 12.5mm and 25mm in the bed of gypsum board is simulated and a comparison between the different cases is made. In order to compare the results of the different simulations, Figure 4 proposes five parameters derived from a typical temperature and RH response inside gypsum board at a depth of 12.5mm to a step change in relative humidity (step change from 30%RH to 71.9%RH, and back to 29.6%RH). ΔRHa indicates the magnitude of change in relative humidity after an adsorption phase. ΔRHd is the magnitude of RH change during a desorption phase. RHmax gives the maximum simulated relative humidity. Tmax stands for the maximum simulated temperature and Tmin for the minimum temperature. A similar approach was used in Annex 41. For all simulations the boundary and inlet conditions are the same. As a result the effect of material properties can be revealed.

Table 3 lists the simulated values for ΔRHa, ΔRHd and RHmax at a depth of 12.5mm and 25mm. Table 4 does the same but for the simulated maximum temperature Tmax and the minimum temperature Tmin. Results for the reference case are shown in the first row of Table 3 and 4. When the relative humidity of the supplied air is changed from 30% to 71.9%, vapour diffuses from the moist air to the drier porous material. During this adsorption phase, the relative humidity inside the material rises (as well as the moisture content). For the reference case the relative humidity reaches its highest value of 68.02% at a depth of 12.5mm and 65.64% at a depth of 25mm before the relative humidity of the supplied air is lowered again. Hygroscopic materials like gypsum board store liquid moisture at a relative humidity below 100%. At low relative humidity (RH<40%) water molecules are adsorbed/desorbed at the porous walls which is accompanied by a heat of adsorption. As mentioned before, in this model the heat of adsorption is assumed to be equal to the heat of vaporization. Hence, even though the relative humidity in the surrounding air is only 71.9%, part of the water vapour entering the gypsum board will condense in the in the pores. This phase change in accompanied by latent heat release which explains the shape of the temperature curve on Figure 4. During the adsorption phase, water vapour condenses in the hygroscopic material resulting in a temperature rise in the material. During the desorption phase water vapour evaporates from the material which requires energy. As a result the temperature inside the gypsum board drops.

5.1. Density, thermal conductivity and heat capacity variations

The reference case is compared to the cases with different material properties. These simulations clearly show that changes of 5% in dry density, thermal conductivity and heat capacity have virtually no effect on the model outcome regarding both temperature and relative humidity. The same results were also found by [20]. Olutimayin et al. measured and modelled heat and moisture transfer in cellulose insulation. He also performed a sensitivity analysis but changed the material properties by 10% in stead of 5%. Still he concluded that the effect of thermal conductivity on the simulated temperature was less than 1% and could thus be neglected.

5.2. Sorption isotherm and vapour resistance factor variations

Simulations were performed for different sorption isotherms and vapour resistance factors corresponding with the curves shown on Figure 2 and 3. The results of these simulations are shown in Figure 5 and 6.

Figure 5 shows that a higher sorption isotherm (w+) results in a decrease of the maximum relative humidity by 1.72% points and a decrease of the sorption isotherm (w-) results in a relative humidity increase by 0.94% points. These values are relatively low compared to the differences between the sorption isotherms. A variation of the sorption isotherm also affects the simulated temperature. The temperature change due to latent heat effects is slightly smaller for a lower sorption isotherm and slightly larger for a higher sorption isotherm. These results correspond with what can be physically expected. An increased sorption isotherm will result in higher moisture content and higher specific moisture content ($\partial w/\partial RH$). This means that the same moisture content would correspond with a lower relative humidity or, more vapour would have to diffuse into the porous material to reach the same relative humidity. In other words it will take a longer time for the air in the porous material to reach a certain relative humidity. The temperature variation due to

the phase change increases because more vapour condenses during adsorption and evaporates during desorption.
Talukdar et al. [18] performed a similar study for spruce plywood and applied a ±10% variation for each material property. They found similar results. Increasing the sorption isotherm with 10% resulted in a reduction of the relative humidity by 6% relative to the applied step change, which was 50%RH. A reduction of the sorption isotherm increased the relative humidity by 6% relative to the step change. They found that the difference between the measured and the simulated values for relative humidity were typically smaller than the fluctuations they found for different sorption isotherms. They concluded that the sorption isotherm they used for the modelling agreed well with reality.
Changing the vapour resistance factor by a higher or lower curve also changes the model outcome (see Figure 6). Similar to the higher sorption isotherm, a higher vapour resistance factor results in a lower relative humidity during the adsorption phase and a higher relative humidity during the desorption phase. The opposite counts for a lower vapour resistance factor. Again, the effect is more pronounced deeper in the material.
A higher vapour resistance factor corresponds to a lower vapour permeability. Thus it is more difficult for the water vapour to penetrate the porous material. This explains why a lower relative humidity is found during adsorption and a higher relative humidity is found during desorption. Simultaneously the temperature change due to the latent heat effect is less pronounced for a higher vapour resistance factor and the other way around for a lower vapour resistance factor.
However, in reality the sorption isotherm and vapour resistance factor do not change independently and are both function of the pore structure. To investigate the combined effect of a changed sorption isotherm and vapour permeability, four simulations were performed: high sorption with high vapour resistance (w+ μ+), high sorption with low vapour resistance (w+ μ-), low sorption with high vapour resistance (w- μ+) and low sorption with low vapour resistance (w- μ-). The results of these simulations are shown in Figure 7. Again a higher sorption isotherm (associated to a larger moisture capacity) results in a lower relative humidity during adsorption and a higher relative humidity during desorption. In other words this will dampen the humidity variation in the material. Combining this higher sorption isotherm with a higher vapour resistance will further reduce the amplitude of the humidity change in the material. On the other hand, the combination with a lower vapour resistance will counter the effect which explains why the curve for w+ μ- does not differ much from the reference simulation.
Similar effects are found for a lower sorption isotherm combined with a higher vapour resistance. A lower sorption isotherm will result in a higher relative humidity during adsorption and a lower relative humidity during desorption. A combination with a higher vapour resistance (w- μ+) will reduce the effect and will result again in a relative humidity curve that does not differ a lot from the reference case. On the other hand, a combination with a lower vapour resistance (w- μ-) will intensify the relative humidity increase/decrease. In other words, the relative humidity change in a material is damped by a higher moisture capacity and slowed down by a lower permeability (higher vapour resistance).
Also the temperature is influenced by a change in sorption and/or permeability. This is shown in Figure 7 (b) and (d). Unlike the relative humidity response, the largest effect is found for w+ μ- and w- μ+. A low vapour resistance means that vapour easily diffuses

into or out of the material. A combination with a high sorption means that this vapour is easily stored by the material in the liquid phase. So more water vapour will condense/evaporate resulting in an increased latent heat effect. A high vapour resistance and a low sorption isotherm results in a reduced latent heat effect.
With respect to the latent heat effects, a high sorption isotherm and high vapour resistance (w+ μ+) counteract each other. A high sorption (and higher moisture capacity) will increase the latent heat effect, a higher vapour resistance (lower permeability) will reduce the latent heat effect.
Note that the combination of the sorption isotherms and the vapour resistance factors is arbitrary and does not necessarily correspond with a real material. To find out if similar conclusions still hold for real materials two extra simulations were performed on two other materials. The first material is calcium silicate (CaSi). This material has a higher sorption isotherm than gypsum board and also a higher permeability. The second material is ceramic brick, which has a much lower permeability and sorption isotherm than the gypsum board. The material properties for these cases were taken from [21]. To model the sorption isotherm and the vapour resistance, again the analytical functions given by Equation (11) and (12) are used. The corresponding coefficients are found in Table 5. The simulation results are shown in Table 3 and 4 and in Figure 8. For CaSi almost no change in relative humidity is found. A higher sorption isotherm and a higher permeability counter each other with respect to the relative humidity response of the material. However, more vapour condenses in the CaSi during adsorption resulting in a higher latent heat effect. These results correspond with the previously discussed w+μ- case.
Ceramic brick has a much higher vapour resistance and a lower sorption isotherm than gypsum board. This results in almost no temperature change due to latent heat effect in the material. These results correspond with the w-μ+ case. However, due to the much lower sorption isotherm, less water condenses inside the material and the relative humidity inside the material is less damped due to the lower moisture capacity. These simulations prove that the model predicts the correct trends.

5.3. Influence of air velocity, transfer coefficients, inlet temperature and relative humidity.

Simulation results shown up till now were all computed with laminar flow conditions. The average inlet velocity of 0.82m/s corresponds with Re=2000. Increasing the Reynolds number to 5000, and thus increasing the average velocity, results in a turbulent flow over the gypsum sample. Increasing the Reynolds number will also increase the transfer coefficients for heat and mass. Nevertheless, when analyzing the results in Table 3 and 4 it is clear that this higher mass transfer coefficient has almost no effect on the response of the relative humidity inside the material. Mass transfer between the air and the porous materials is thus obviously dominated by the vapour diffusion resistance and not by the mass transfer coefficient. The same conclusions were also drawn in subtask 2 of Annex 41 [16] where a change of 10% in the mass transfer coefficient had no significant effect.
Increasing the heat transfer coefficient leads to changes in the temperature response. In case of a higher heat transfer coefficient, the temperature change due to the latent heat effect is damped out due to the better heat transfer from the material to the air.

Two more boundary conditions can be considered: the inlet temperature and inlet relative humidity. These conditions were measured during the experiments and are accompanied by an uncertainty. For the temperature this uncertainty was 0.1°C, for relative humidity this uncertainty was 2%RH. An under- or overestimation of these boundary conditions will affect the model results. To evaluate the impact of an incorrect boundary condition estimation, simulations with altered inlet conditions were performed (inlet temperature ±0.1°C, inlet relative humidity ±2%). The results of these simulations are found in Table 3 and 4. Changing these parameters clearly has a direct impact on the model outcome. Changes to the inlet temperature only affect the temperature result inside the material and have almost no effect on the relative humidity in the material. However, changing the inlet relative humidity affects both temperature and relative humidity. A higher inlet relative humidity will result in a higher relative humidity inside the material, but also a higher latent heat effect in the material, because more water vapour will condense.

5.4. Hysteresis versus no hysteresis modelling

For most porous materials there is no unique relationship between the moisture content and the relative humidity because hysteresis occurs during the sorption/desorption process. The material will behave differently during adsorption and desorption. Therefore a hysteresis model based on the 'ink bottle effect' was included in the coupled CFD-HAM model. This model was originally proposed by Mualem [22] and then later simplified by Milly [23]. A more detailed explanation of this model is found in [12].

The reference case discussed in this paper was validated elaborately in [12]. Measured temperature and relative humidity at a depth of 12.5mm and 25mm in the gypsum board are plotted on Figure 8. The uncertainties on the measurements were ±2% for relative humidity and ±0.1°C for temperature. No perfect match between the measured and simulated relative humidity was found, but the results were still acceptable. To obtain a better agreement between the model and the experiment, the relative humidity should be higher during the adsorption phase and lower during the desorption phase. Figure 9 shows that the agreement is better at a depth of 12.5mm than at 25mm.

Implementing a hysteresis model improves the predicted relative humidity during the desorption phase. This is in agreement with the expectations. The hysteresis model uses a desorption isotherm during the desorption phase which has higher values for moisture content than the adsorption isotherm at the same relative humidity. As a result, implementing a hysteresis model gives similar results during desorption as the lower isotherm (w_a-) in Figure 2. Combining a lower sorption isotherm with hysteresis result in an even better agreement, also during the adsorption phase as would be expected.

The agreement between the simulated and measured temperatures is rather poor. Strange fluctuations in the measured temperature are found which could be explained by the fluctuating inlet temperature. Although the test setup was designed to supply a constant inlet temperature, reality showed that this was not always the case. Inaccurate positioning of the thermocouples and RH sensors could also explain some of the deviations. Therefore it is hard to conclude whether the model has good agreement for temperature or not.

5.5. Modelling gypsum board as layered

Gypsum board is built up out of multiple layers but modelled as a uniform material which could affect the simulations. The gypsum board used in this study has a thickness of

12.5mm and consists out of three layers: a layer of finishing paper at both sides (thickness 0.5mm) and a layer of gypsum in between (thickness 11.5mm). Roels et al. [24] measured the material properties for each layer separately. The sorption isotherm and the vapour resistance factor for paper and gypsum are given by equations (13) and (14). The corresponding coefficients are listed in Table 6. No hysteresis is considered so only the adsorption isotherm is considered.

$$w = w_{sat}\left(1 + \left(-a\rho_w R_v T \ln(RH)\right)^n\right)^{(1-n)/n} \tag{13}$$

$$\mu = \frac{1}{a + b\exp(cRH)} \tag{14}$$

Here ρ_w represents the water density (998.2 kg/m³) and R_v is the specific gas constant for water vapour (462 J/kgK).
Figure 10 shows some simulation results for relative humidity and temperature in the gypsum board for uniform modelling and layered modelling. These results differ from the reference case because a slightly different sorption isotherm and vapour resistance has been used: the curves used here are the ones measured by Roels et al. [21] and correspond to the lower curves in Figure 2 and Figure 3. This explains why the predicted relative humidity is higher during adsorption and lower during desorption. The difference in simulated relative humidity and temperature for the uniform and layered modelling is negligibly small. By consequence modelling the gypsum board as layered has limited impact on the model outcome.

6. Conclusions

An extensive sensitivity analysis was performed on a recently developed coupled CFD-HAM model. This model uses CFD to calculate the indoor air distributions around a porous material and combines this with a HAM model to incorporate the heat and mass transfer between air and the porous material. By using a direct coupling method, no external data exchange between the two models is needed which increases the computational speed of the model.
Data from a benchmark transient heat and mass transfer experiment performed during IEA Annex 41 were used as a reference case for the sensitivity analysis. The material data used for this case were the average values found in a round robin test which was also performed during IEA Annex 41. This test showed that large discrepancies could occur between material properties measured at different laboratories.
In this paper it is shown that the coupled CFD-HAM model is rather insensitive to deviations of most of the material properties. For density, heat capacity and thermal conductivity of the porous material no significant effect on simulated temperature and relative humidity was found when these properties were changed by 5%. The impact of sorption isotherm and vapour resistance factor was more severe. These properties are often harder to measure, resulting in large uncertainties. Deviations in the simulated relative humidity up to 2%RH were found for the different isotherms and resistance factors. These hygroscopic properties also have an impact on the calculated temperature although this effect is limited.

Increasing the air velocity from laminar to turbulent had no effect on the relative humidity inside the porous material because the diffusive mass transfer dominates over the convective mass transfer. This is however not the case for temperature, where the impact of the convective heat transfer coefficient is of more importance.
The effect of hysteresis modelling was also investigated in this paper. Including hysteresis in the model improved the model outcome, though it is not sufficient to get a full agreement with measurement data. These deviations can now be explained by the sensitivity analysis. A large uncertainty of the material property data, especially of the sorption isotherm and the vapour resistance leads to deviations in the modelling outcome. The combined effect of an uncertainty on the sorption isotherm and on the vapour resistance can lead in some cases to even greater deviations in the model. These effects are large enough to explain why the model does not fully match the measurements.
Finally, modelling gypsum board as a layered material showed to have no impact on the results.
This paper shows that the model works well and that its accuracy is to a great extent determined by the accuracy of the input data and material properties. For the moisture transfer modelling this data is still accompanied by large inaccuracies and even discrepancies between laboratories which means that more research is certainly needed.

7. Acknowledgement

The results presented in this paper have been obtained within the frame of the IWT SBO-050451 project "Heat, air and moisture performance engineering a whole building approach" and the Flemish Institute for the Promotion and Innovation by Science and Technology in Flanders (IWT-SB/81322/Van Belleghem). Their financial support is gratefully acknowledged.

8. Nomenclature

a	Coefficient in sorption isotherm or vapour resistance factor
b	Coefficient in sorption isotherm or vapour resistance factor
c	Coefficient in sorption isotherm
C	Specific heat capacity (J/kgK)
D	Vapour diffusion coefficient in air (m²/s)
d	Thickness (m)
E	Internal energy (J)
g	Vapour diffusion flux (kg/m²s)
L_{vap}	Latent heat of vaporization (J/kg)
n	Coefficient in sorption isotherm
RH	Relative Humidity (%)
ΔRHa	Magnitude of change in relative humidity after an adsorption phase (%)
ΔRHd	Magnitude of change in relative humidity after a desorption phase (%)
RHmax	Maximum relative humidity (%)
Re	Reynolds number (-)
R_v	Specific gas constant of water vapour (J/kgK)
T	Temperature (K)
t	Time (s)

v	Velocity (m/s)
w	Volumetric moisture content in porous material (kg/m³)
w+	High limit for sorption isotherm curve
w-	Low limit for sorption isotherm curve
Y	Mass fraction of water vapour (-)

Greek symbols

Φ	Open porosity (-)
λ	Thermal conductivity (W/mK)
μ	Vapour diffusion resistance factor (-)
$\mu+$	High limit for vapour diffusion resistance factor curve (-)
$\mu-$	Low limit for vapour diffusion resistance factor curve (-)
μ_0	Vapour diffusion resistance factor for dry material
ρ	Density (kg/m³)

Subscripts

a	Adsorption
air	Dry air
d	Desorption
liq	Liquid water
mat	Dry material
max	Maximum
min	Minimum
sat	Saturation
vap	Water vapour

9. References

[1] Pavlogeorgatos G. Environmental parameters in museums. Building and Environment 2003;38(12):1457-1462.
[2] Osanyintola OF, Simonson CJ. Moisture buffering capacity of hygroscopic building materials: Experimental facilities and energy impact. Energy and Buildings 2006;38(10):1270-1282.
[3] Simonson CJ, Salonvaara M, Ojanen T. The effect of structures on indoor humidity - possibility to improve comfort and perceived air quality. Indoor Air 2002;12(4):243-251.
[4] Steeman M, Janssens A, De Paepe M. Performance evaluation of indirect evaporative cooling using whole-building hygrothermal simulations. Applied Thermal Engineering 2009;29(14-15):2870-2875.
[5] Woloszyn M, Kalamees T, Olivier Abadie M, Steeman M, Sasic Kalagasidis A. The effect of combining a relative-humidity-sensitive ventilation system with the moisture-buffering capacity of materials on indoor climate and energy efficiency of buildings. Building and Environment 2009;44(3):515-524.
[6] Hens H. IEA Annex 24. Heat, Air and Moisture Transport, Final report, vol.1, Task 1: modelling. 1996.
[7] Woloszyn M, Rode C. IEA Annex 41. Whole Building Heat, Air and Moisture Response. Subtask1: Modelling Principles and Common Exercises. 2008.

[8] Steeman HJ, Janssens A, Carmeliet J, De Paepe M. Modelling indoor air and hygrothermal wall interaction in building simulation: Comparison between CFD and a well-mixed zonal model. Building and Environment 2009;44(3):572-583.
[9] Kwiatkowski J, Woloszyn M, Roux J-J. Modelling of hysteresis influence on mass transfer in building materials. Building and Environment 2009;44(3):633-642.
[10] Steeman M, Janssens A, Steeman HJ, Van Belleghem M, De Paepe M. On coupling 1D non-isothermal heat and mass transfer in porous materials with a multizone building energy simulation model. Building and Environment 2010;45:865-877
[11] Mortensen LH, Woloszyn M, Rode C, Peuhkuri R. Investigation of microclimate by CFD modeling of moisture interactions between air and constructions. Journal of Building Physics 2007;30(4):279-315.
[12] Steeman HJ, Van Belleghem M, Janssens A, De Paepe M. Coupled simulation of heat and moisture transport in air and porous materials for the assessment of moisture related damage. Building and Environment 2009;44(10):2176-2184.
[13] Steeman HJ, T'Joen C, Van Belleghem M, Janssens A, De Paepe M. Evaluation of the different definitions of the convective mass transfer coefficient for water evaporation into air. International Journal of Heat and Mass Transfer 2009;52(15-16):3757-3766.
[14] Steeman HJ, Janssens A, De Paepe M. On the applicability of the heat and mass transfer analogy in indoor air flows. International Journal of Heat and Mass Transfer 2009;52(5-6):1431-1442.
[15] Hens H. IEA Annex 14: Condensation and Energy, vol.3: Catalogue of Material Properties. 1991.
[16] Roels S. IEA Annex 41. Whole Building Heat, Air and Moisture response. Subtask 2: Experimental Analysis of Moisture Buffering. International Energy Agency, 2008.
[17] Roels S, Carmeliet J, Hens H, Adan O, Brocken H, Cerny R, Pavlik Z, Hall C, Kumaran K, Pel L, Plagge R. Interlaboratory Comparison of Hygric Properties of Porous Building Materials. Journal of Thermal Envelope and Building Science 2004;27(4):307-325.
[18] Talukdar P, Olutmayin SO, Osanyintola OF, Simonson CJ. An experimental data set for benchmarking 1-D, transient heat and moisture transfer models of hygroscopic building materials. Part I: Experimental facility and material property data. International Journal of Heat and Mass Transfer 2007;50(23-24):4527-4539.
[19] Iskra CR, Simonson CJ. Convective mass transfer coefficient for a hydrodynamically developed airflow in a short rectangular duct. International Journal of Heat and Mass Transfer 2007;50(11-12):2376-2393.
[20] Olutimayin SO, Simonson CJ. Measuring and modeling vapor boundary layer growth during transient diffusion heat and moisture transfer in cellulose insulation. International Journal of Heat and Mass Transfer 2005;48(16):3319-3330.
[21] Roels S, Carmeliet J, Hens H, HAMSTAD WP1: Final report – Moisture transfer properties and materials characterisation. Laboratory of Building Physics, KULeuven, 2003.
[22] Mualem Y. Conceptual Model of Hysteresis. Water Resources Research 1974;10(3):514-520.
[23] Milly P. The coupled transport of water and heat in a vertical soil column under atmospheric excitation, PhD thesis, Massachusetts Institute of Technology, 1980.

[24] Roels S, Janssen H, Carmeliet J, Diepens J, de Wit M. Hygric buffering capacities of uncoated and coated gypsum board. Research in Building Physics and Building Engineering - Proceedings of the Third International Building Physics Conference Montreal, Canada, 2006.

Figure 1. Reference case setup

Figure 2. Sorption isotherms for gypsum board (data from [16]) (a) and measured differences between the curves (b). Full lines in (a) correspond with equation (10), x, + and o correspond with measurements.

Figure 3. Vapour resistance factors for gypsum board (data from [16]) (a) and measured differences between the curves (b). Full lines in (a) correspond with equation (12), x, + and o correspond with measurements.

Figure 4. Typical response of the temperature (a) and relative humidity (b) in gypsum board at a depth of 12.5mm for a step change induced in the relative humidity of the surrounding air (29.6%RH-71.9%RH).

Figure 5. Effect of variation in sorption isotherm on the model outcome. Relative humidity at a depth of 12.5mm in the gypsum board(a). Temperature at a depth of 12.5mm (b). Relative humidity at 25mm (c). Temperature at 25mm (d).

Figure 6. Effect of variation in vapour resistance factor on model outcome. Relative humidity at a depth of 12.5mm in the gypsum board (a). Temperature at a depth of 12.5mm (b). Relative humidity at 25mm (c). Temperature at 25mm (d).

Figure 7. Combined effect of sorption isotherm and vapour resistance factor. Relative humidity at a depth of 12.5mm in the gypsum board (a). Temperature at a depth of 12.5mm (b). Relative humidity at 25mm (c). Temperature at 25mm (d).

Figure 8. Comparison of the model results for CaSi, brick and gypsum board (same boundary and inlet conditions).

Figure 9. Comparing the model with hysteresis and without at a depth of 12.5mm (a,b) and 25mm (c,d) for relative humidity and temperature.

Figure 10. Modelling gypsum board as a uniform material or layered. Temperature and relative humidity at a depth of 12.5mm (a,b) and 25mm (c,d).

Table 1. Material properties gypsum board

Table 2. Coefficients for sorption isotherms and vapour resistance factor of gypsum board

Table 3. Relative humidity change in the adsorption phase ΔRHa, relative humidity change in the desorption phase ΔRHd and the maximum relative humidity RHmax at a depth of 12.5mm and 25mm

Table 4. Maximum temperature Tmax and minimum temperature Tmin during simulation at a depth of 12.5mm and 25mm

Table 5. Material properties of calcium silicate and ceramic brick adopted from [21]

Table 6. Coefficients for the sorption isotherm and vapour resistance factor of finishing paper and gypsum [24]

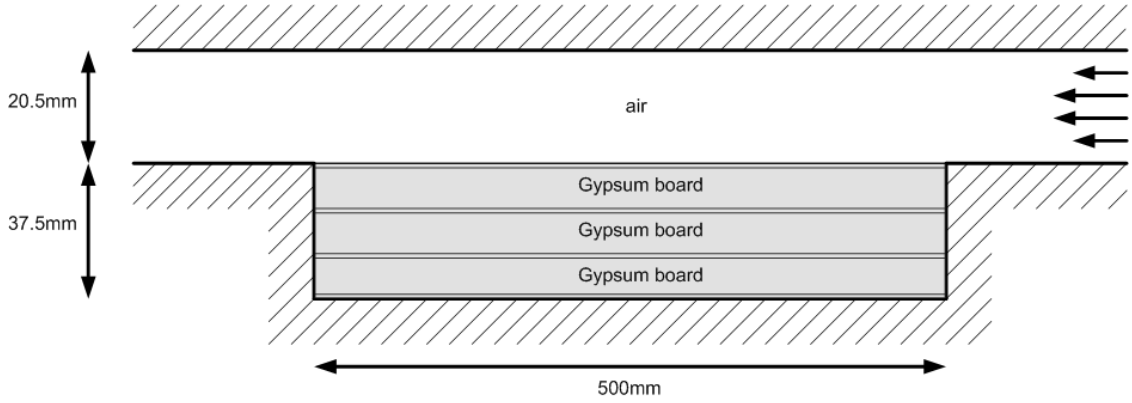

Figure 1. Reference case setup

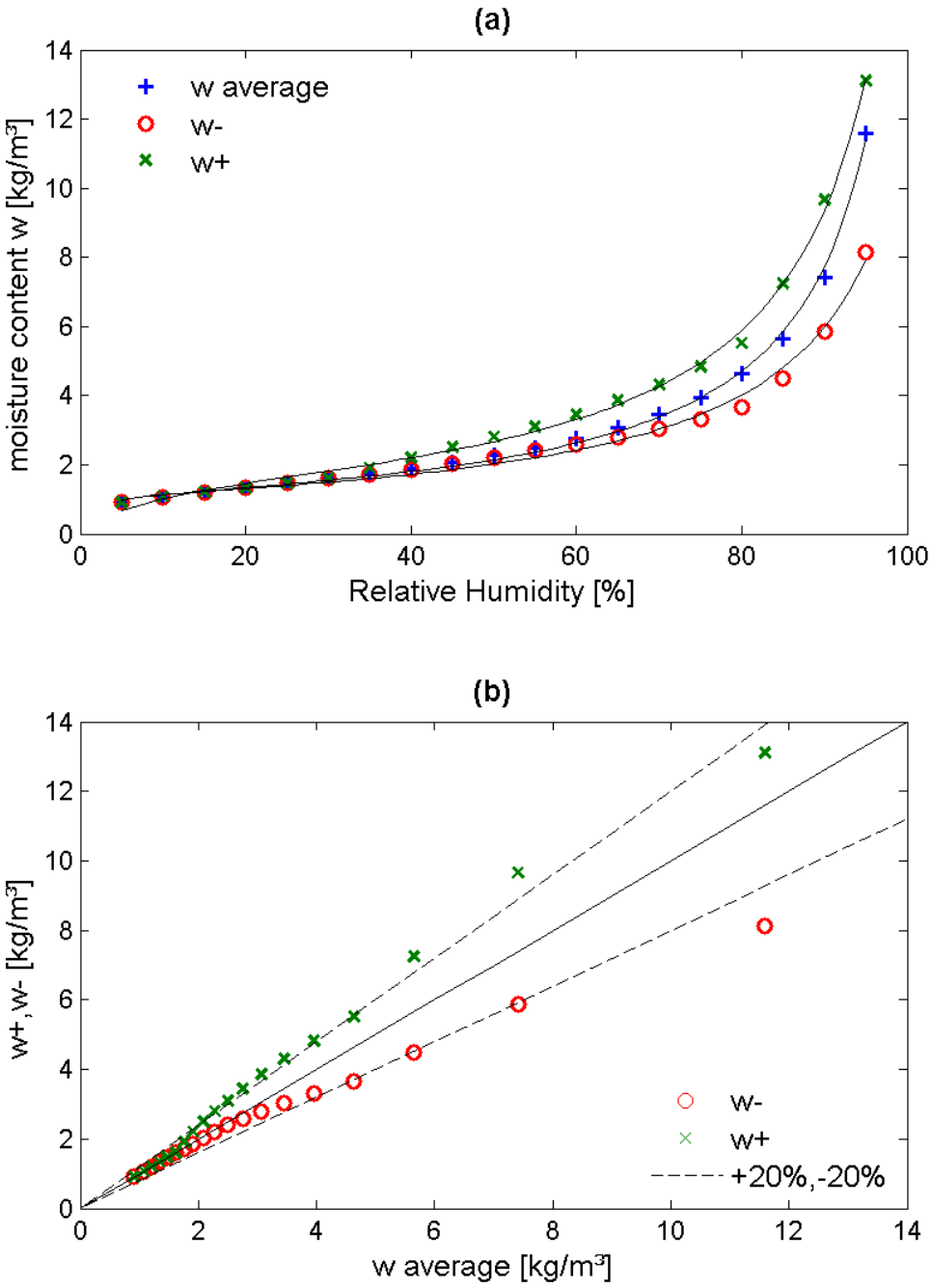

Figure 2. Sorption isotherms for gypsum board (data from [16]) (a) and measured differences between the curves (b). Full lines in (a) correspond with equation (10), x, + and o correspond with measurements.

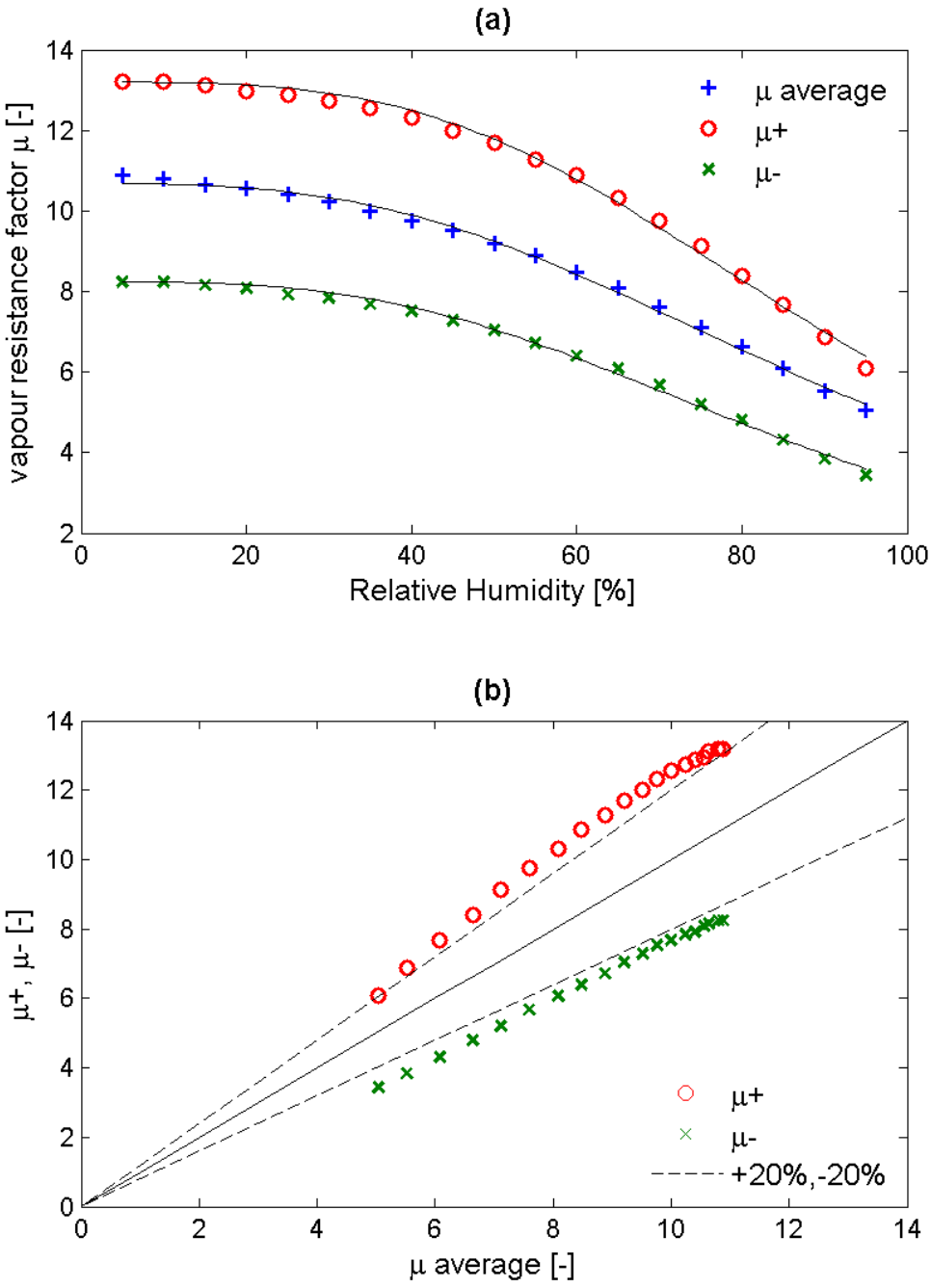

Figure 3. Vapour resistance factors for gypsum board (data from [16]) (a) and measured differences between the curves (b). Full lines in (a) correspond with equation (12), x, + and o correspond with measurements.

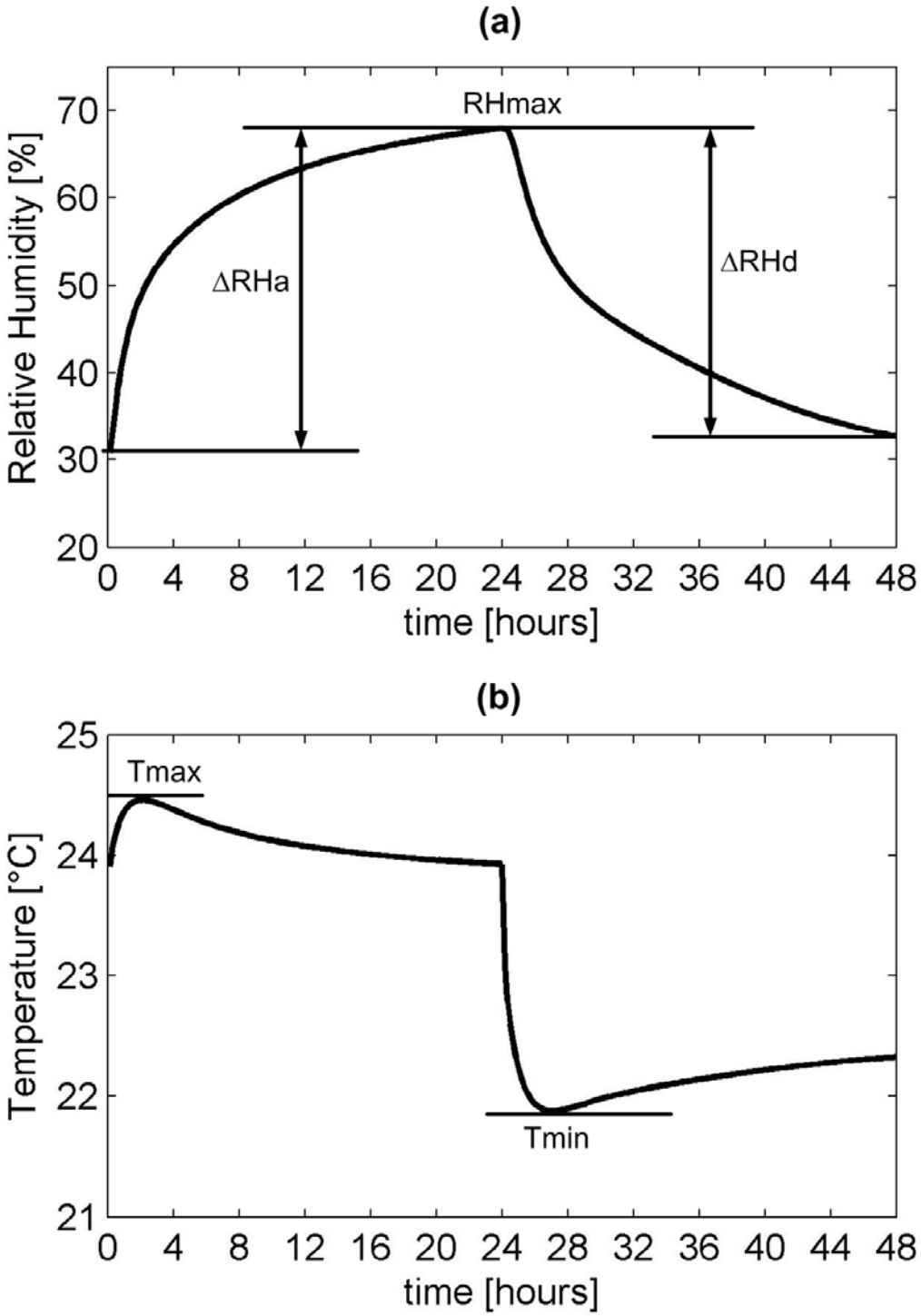

Figure 4. Typical response of the temperature (a) and relative humidity (b) in gypsum board at a depth of 12.5mm for a step change induced in the relative humidity of the surrounding air (29.6%RH-71.9%RH).

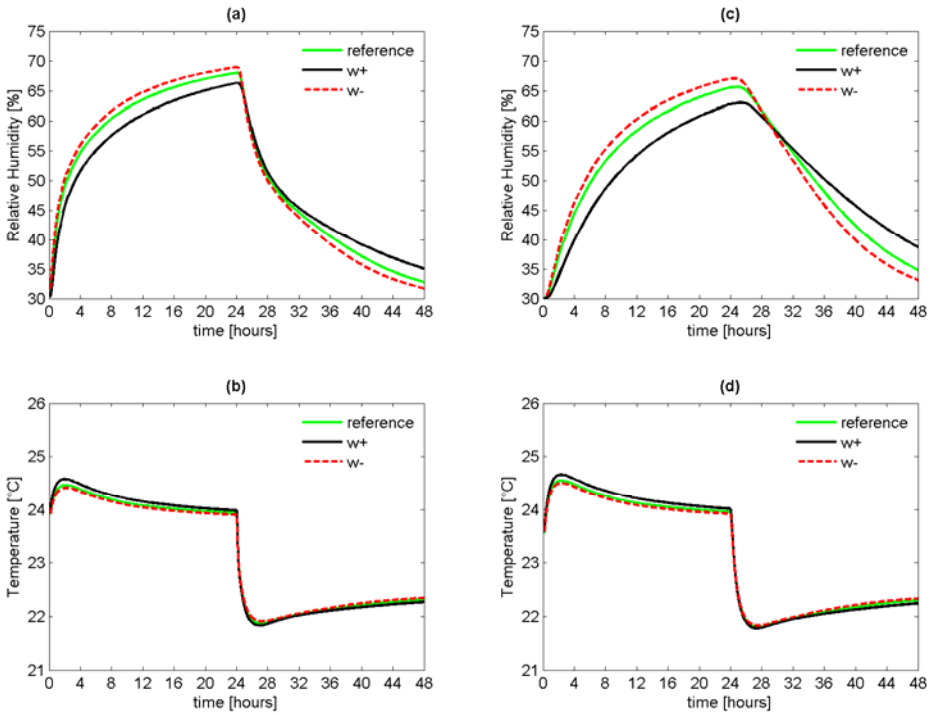

Figure 5. Effect of variation in sorption isotherm on the model outcome. Relative humidity at a depth of 12.5mm in the gypsum board(a). Temperature at a depth of 12.5mm (b). Relative humidity at 25mm (c). Temperature at 25mm (d).

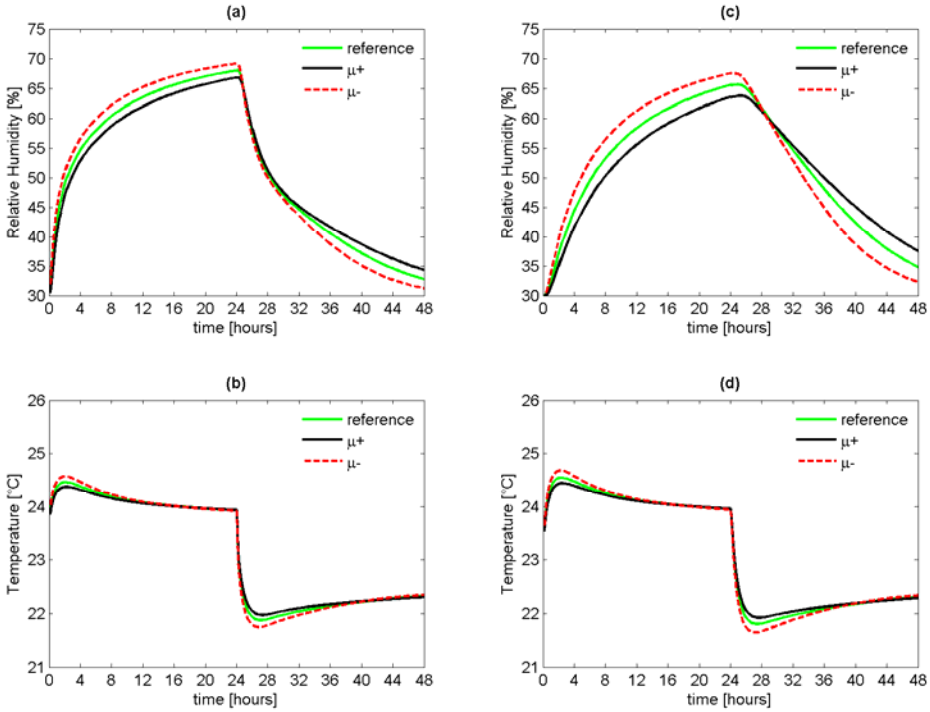

Figure 6. Effect of variation in vapour resistance factor on model outcome. Relative humidity at a depth of 12.5mm in the gypsum board (a). Temperature at a depth of 12.5mm (b). Relative humidity at 25mm (c). Temperature at 25mm (d).

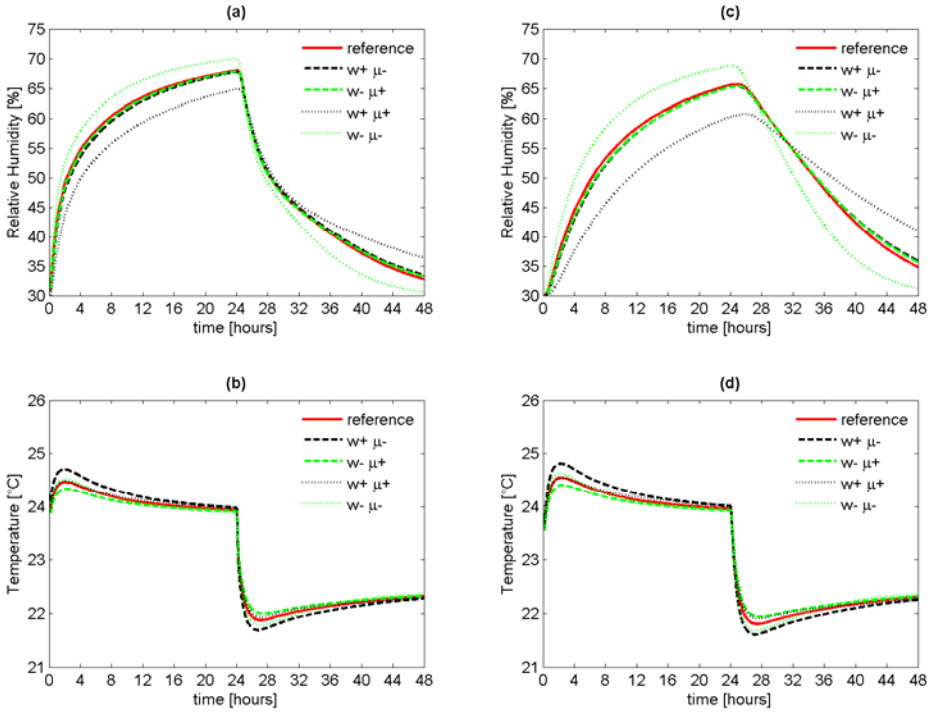

Figure 7. Combined effect of sorption isotherm and vapour resistance factor. Relative humidity at a depth of 12.5mm in the gypsum board (a). Temperature at a depth of 12.5mm (b). Relative humidity at 25mm (c). Temperature at 25mm (d).

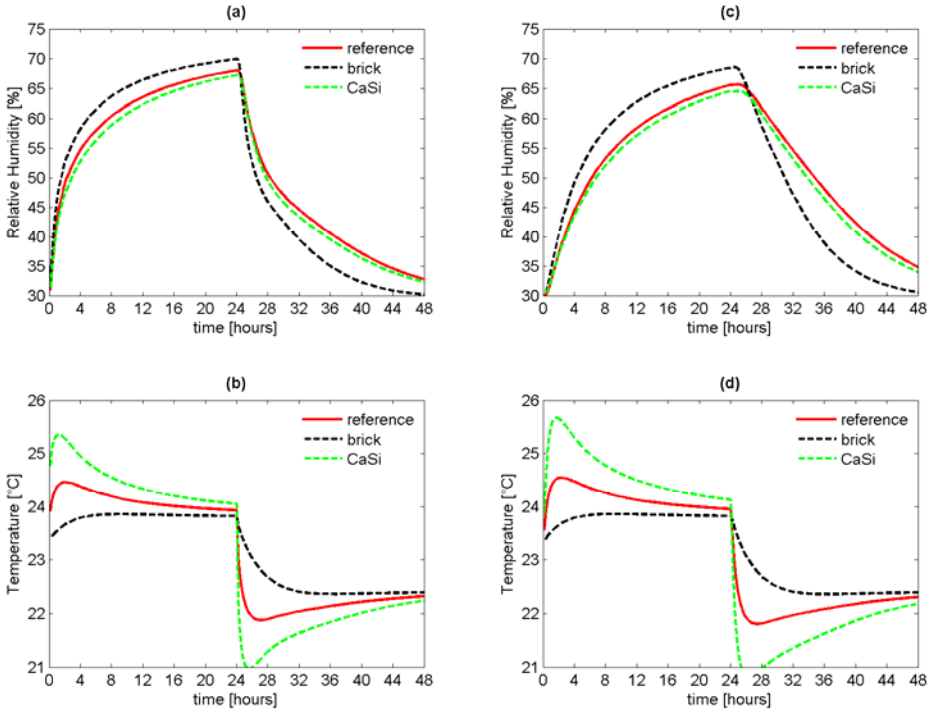

Figure 8. Comparison of the model results for CaSi, brick and gypsum board (same boundary and inlet conditions).

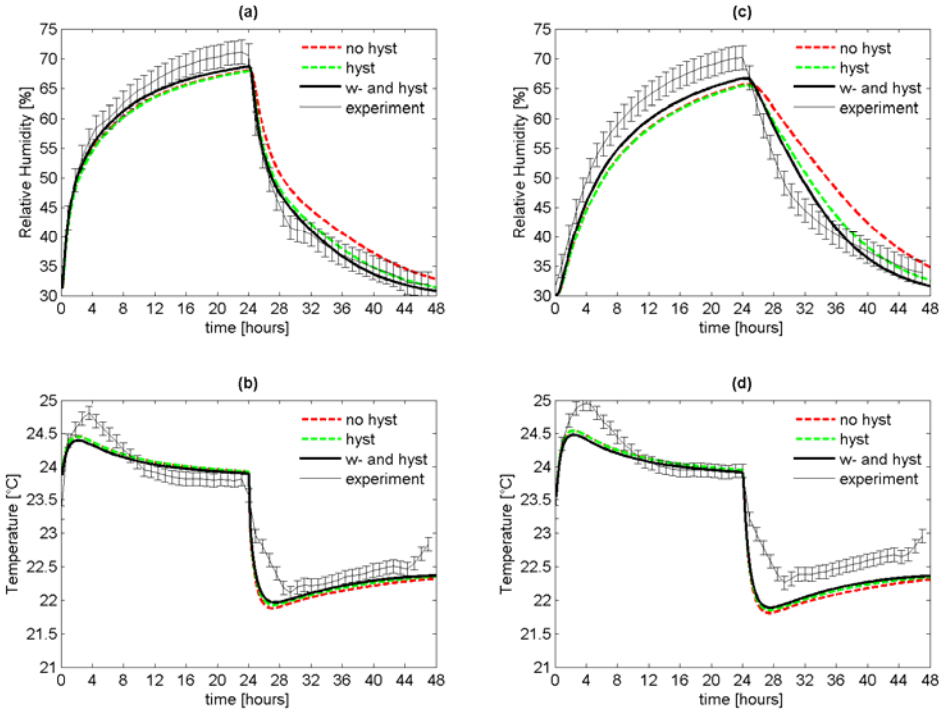

Figure 9. Comparing the model with hysteresis and without at a depth of 12.5mm (a,b) and 25mm (c,d) for relative humidity and temperature.

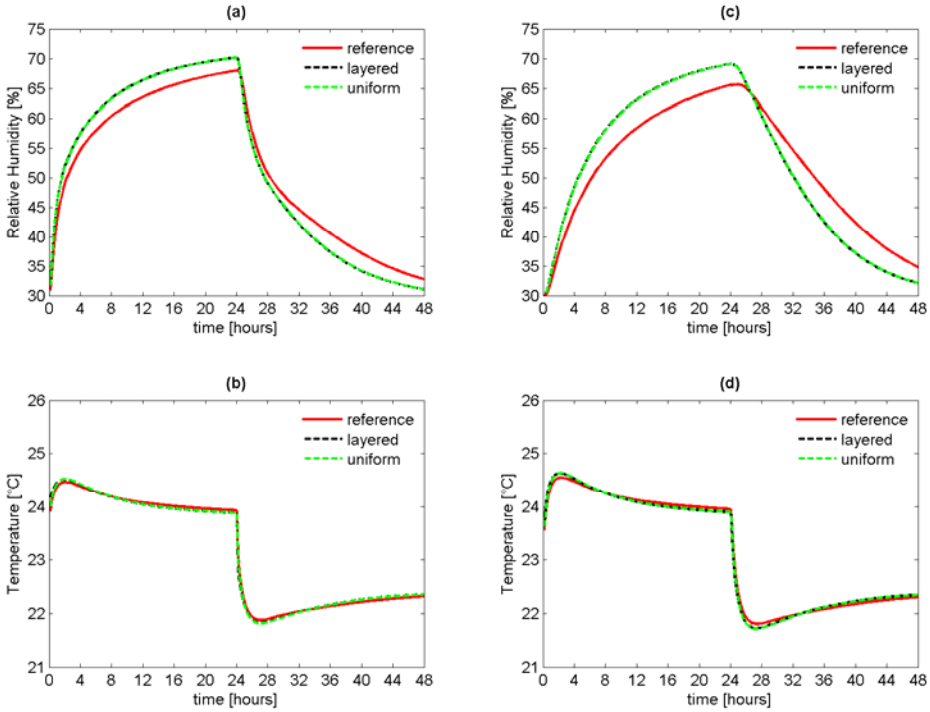

Figure 10. Modelling gypsum board as a uniform material or layered. Temperature and relative humidity at a depth of 12.5mm (a,b) and 25mm (c,d).

Table 1. Material properties gypsum board

Material property	unit	Reference value	Min (-5%)	Max (+5%)
Thickness d	m	0.0125	-	-
Density ρ	kg/m³	690	655.5	724.5
Open porosity Φ	-	0.419	0.448	0.39
Thermal conductivity λ	W/mK	0.198	0.188	0.208
Heat capacity C_{mat}	J/kgK	840	798	882

Table 2. Coefficients for sorption isotherms and vapour resistance factor of gypsum board

	+	Average	-
Absorption isotherm w_a gypsum board			
a	-0.562516742	-0.81655	-0.8054748
b	0.560112656	0.85157	0.883480733
c	0.047583587	0.011176	0.007663124
Desorption isotherm w_d gypsum board			
a		13.91382	
b		0.079139	
c		1.944272	
Vapour resistance factor gypsum board			
μ_0	13.2	10.68205	8.24
a	1.268102	1.229557	1.512357696
n	3.392995	2.983921	3.174273855

Table 3. Relative humidity change in the adsorption phase ΔRHa, relative humidity change in the desorption phase ΔRHd and the maximum relative humidity RHmax at a depth of 12.5mm and 25mm

	@12.5mm			@25mm		
	ΔRHa[%]	ΔRHd[%]	RHmax[%]	ΔRHa[%]	ΔRHd[%]	RHmax[%]
Reference case	38.02	35.31	68.02	35.64	30.83	65.64
Experiment	41	40.2	71.5	38.9	36.4	69.1
ρ+5%	38.02	35.32	68.02	35.64	30.84	65.64
ρ-5%	38.02	35.31	68.02	35.64	30.83	65.64
λ+5%	38.02	35.32	68.02	35.66	30.86	65.66
λ-5%	38.01	35.30	68.01	35.62	30.80	65.62
C_{mat}+5%	38.02	35.32	68.02	35.64	30.84	65.64
C_{mat}-5%	38.02	35.31	68.02	35.64	30.83	65.64
Sorption isotherm +	36.30	31.27	66.30	33.03	24.32	63.03
Sorption isotherm -	38.96	37.26	68.96	37.07	33.96	67.07
μ+	36.84	32.58	66.84	33.77	26.27	63.77
μ-	39.18	37.97	69.18	37.51	35.45	67.51
w + μ -	37.77	34.38	67.77	35.32	29.43	65.32
w - μ +	37.88	34.74	67.88	35.35	29.76	65.35
w + μ +	34.87	28.56	64.87	30.73	19.80	60.73
w - μ -	39.99	39.46	69.99	38.79	37.65	68.79
RH+2%	39.54	34.45	69.54	36.95	29.49	66.95
RH - 2%	36.38	36.09	66.38	34.21	32.09	64.21
T + 0.1°C	38.01	35.98	68.01	35.65	31.57	65.65
T - 0.1°C	37.94	35.23	67.94	35.55	30.71	65.55
Layered	40.18	39.11	70.18	39.12	37.08	69.12
Uniform	40.15	39.07	70.15	39.08	37.01	69.08
Brick	39.90	39.72	69.90	38.52	37.95	68.52
CaSi	37.22	34.99	67.22	34.53	30.58	64.53
Re=5000	38.21	35.66	68.21	35.85	31.24	65.85

Table 4. Maximum temperature Tmax and minimum temperature Tmin during simulation at a depth of 12.5mm and 25mm

	@12.5mm		@25mm	
	Tmax [°C]	Tmin [°C]	Tmax [°C]	Tmin [°C]
Reference case	24.46	21.88	24.54	21.81
Experiment	24.8	22.2	24.9	22.3
ρ+5%	24.44	21.89	24.53	21.82
ρ-5%	24.47	21.86	24.56	21.79
λ+5%	24.46	21.88	24.54	21.81
λ-5%	24.46	21.88	24.55	21.80
C_{mat}+5%	24.44	21.89	24.53	21.82
C_{mat}-5%	24.48	21.86	24.56	21.79
Sorption isotherm +	24.57	21.83	24.66	21.78
Sorption isotherm -	24.41	21.91	24.50	21.83
μ+	24.37	21.97	24.44	21.92
μ-	24.57	21.75	24.68	21.65
w + μ -	24.70	21.69	24.81	21.61
w - μ +	24.33	22.00	24.40	21.94
w + μ +	24.48	21.94	24.54	21.91
w - μ -	24.51	21.79	24.62	21.68
RH+2%	24.51	21.86	24.60	21.79
RH-2%	24.41	21.90	24.50	21.82
T+0.1°C	24.54	21.97	24.63	21.89
T-0.1°C	24.38	21.78	24.46	21.71
Layered	24.51	21.83	24.62	21.72
Uniform	24.52	21.81	24.63	21.71
Brick	23.86	22.36	23.86	22.36
CaSi	25.35	20.97	25.67	20.82
Re=5000	24.34	21.97	24.43	21.90

Table 5. Material properties of calcium silicate and ceramic brick adopted from [21]

		Calcium silicate	**Ceramic brick**
Density ρ (kg/m³)		270	2005
Porosity Φ (-)		0.894	0.157
Thermal conductivity λ (W/mK)		0.06+5.6e-4 w	0.5+4.5e-3 w
Heat capacity C_{mat} (J/kgK)		1000	840
Sorption isotherm			
	a	894	157
	b	0.000254	0.000111
	c	1.38112	1.485996
Vapour resistance factor			
	μ0	5.420218	29.10871
	a	0.053657	-0.00031
	n	31.5258	2.075083

Table 6. Coefficients for the sorption isotherm and vapour resistance factor of finishing paper and gypsum [24]

	Sorption isotherm		
	w_{sat}	a	n
Finishing paper	155	1.35e-6	1.48
Gypsum	130	50.7e-6	1.55
Uniform	130	24.8e-6	1.52
	Vapour resistance factor		
	a	b	c
Finishing paper	0.1	4.78e-3	4.10
gypsum	0.1	4.78e-3	4.10